
ANOVA exemplars for understanding data drift

Sinead A. Williamson

University of Texas at Austin / CognitiveScale

Abstract

The distributions underlying complex datasets, such as images, text or tabular data, are often difficult to visualize in terms of summary statistics such as the mean or the marginal standard deviations. Instead, a small set of exemplars or prototypes—real or synthetic data points that are in some sense representative of the entire distribution—can be used to provide a human-interpretable summary of the distribution. In many situations, we are interested in understanding the *difference* between two distributions. For example, we may be interested in identifying and characterizing data drift over time, or the difference between two related datasets. While exemplars are often more easily understood than high-dimensional summary statistics, they are harder to compare. To solve this problem, we introduce ANOVA exemplars. Rather than independently find exemplars S_X and S_Y for two datasets X and Y , we aim to find exemplars that are both representative of X and Y , and that maximize the overlap $|S_X \cap S_Y|$ between the two sets of exemplars. We can then use the differences between the two sets of exemplars to describe the difference between the distributions of X and Y , in a concise, interpretable manner.

1 Introduction

Data drift—the phenomenon where the distribution underlying our data changes over time—can lead to deterioration in performance of machine learning algorithms. A number of methods have been proposed to measure data drift [1–8], and to describe its nature in broad terms: gradual vs rapid, affecting $P(X)$ or $P(Y|X)$ [9]. However, more specific, user-interpretable ways of conveying the nature of data drift have been under-explored.

Consider a data practitioner faced with a stream of data. It is useful to her to know that the data’s distribution has changed, as this may spur model modifications or retraining [10–12]. Two-sample tests and distributional distances can be used to identify *whether* a distribution has changed, and assess the magnitude or rate of change [8, 13]. However, it is also important that she understands *how* the data has changed. This allows her to ascertain whether the data drift is due to population changes or changes in the sampling mechanism, and determine whether the drift is likely to cause problems in future predictive tasks. If the drift is due to changes in the sampling mechanism, it allows her to identify which sub-populations are being under- or over-represented.

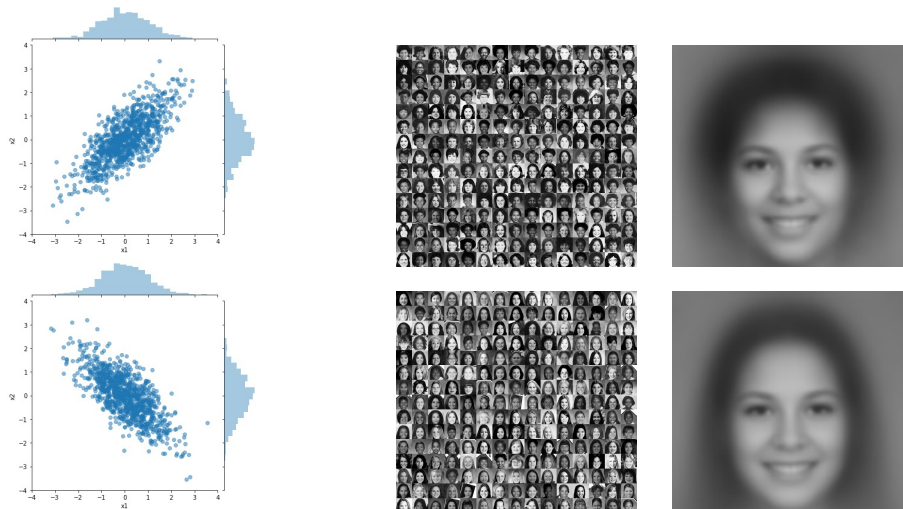
A naïve way of reporting the nature of data drift is to describe differences in the mean and standard deviation of the one-dimensional marginals of the data, or compare histograms [14, 15]. This allows us to see that the number of male observations has increased, or that the variance of users’ heights has increased. However, not all forms of data drift can be captured in this way, since we can change a distribution by changing the correlation structure, without changing the marginals. Comparing higher-dimensional statistics, such as the covariance matrix, can avoid such problems, but the resulting summaries are much harder to interpret. Further, in many contexts both the one-dimensional marginals and higher-order statistics may not be interpretable: Consider distributions over images, where the per-pixel marginals carry little interpretable information, and where the mean image is outside of the data domain.

When describing a single data distribution, one alternative to classical summary statistics is to describe the distribution in terms of a small number of representative points—either exemplars [16, 17], which are subsets of the original data, or prototypes [18], which need not exist in the original dataset. Such representative points can be used to summarize a dataset in an easily digestible form. Looking at a small number of data points can allow the user to visualize the nature of the data distribution, even in cases such as images or documents where classical summary statistics are not particularly interpretable.

Intuitively, if two datasets are similar, they can be described using similar exemplars. That similarity can be hard to assess visually, however: even if X and Y have the same underlying distribution, their optimal exemplars typically won't overlap. In this paper, we consider an ANOVA-style decomposition of related datasets into a set of shared exemplars that characterize their similarities, and a set of local exemplars that characterize their differences. We refer to the resulting representative points as ANOVA exemplars.

This leads to a very interpretable method of describing the difference between two datasets. We can directly provide exemplars of the type of data point that have increased, and decreased, in prevalence. Concurrently, we can provide an interpretable summary of both the individual data sets, and their commonalities.

After reviewing existing approaches to data set summarization and comparison, we introduce the idea of ANOVA exemplars in Section 3, and describe an algorithm to learn locally optimal ANOVA exemplars. In Section 4 we give quantitative and qualitative assessments of the exemplars found on both image and document datasets.



(a) Synthetic datasets, with marginal histograms. Comparing marginal distributions and statistics can ignore changes in correlation structure
 (b) Top left: yearbook photos from the 1950s. Bottom left: yearbook photos from the 1970s. Top right: mean image of yearbook photos from the 1950s. Bottom right: mean image of yearbook photos from the 1970s. While the distribution has shifted (see Section 4), it is hard to tell how from the mean.

Figure 1: Looking at summary statistics often obscures differences between two datasets.

2 Related work

Our work falls in the tradition of measuring and characterizing differences between two distributions, based on samples from those distribution. Consider a set of samples $X \sim \mathbb{P}$, and $Y \sim \mathbb{Q}$, for some unknown distributions \mathbb{P} and \mathbb{Q} . We wish to provide low-dimensional, interpretable representations of both the distributions \mathbb{P} and \mathbb{Q} , and of the difference between these distributions. We begin by discussing existing ways of characterizing individual distributions, before looking at existing methods for tracking the difference between those distributions.

2.1 Characterizing distributions

Classical approaches to characterizing an unknown distribution \mathbb{P} in terms of samples $X \sim \mathbb{P}$ rely on calculating summary statistics for X . For example, we can measure the empirical moments of X , which serve as estimators for the moments of \mathbb{P} . However, in high dimensional or highly structured data, such summary statistics can be hard to interpret, and can exclude important information about the distribution [19, 20]. Consider for example a distribution over images (Figure 1b). The per-pixel mean and standard deviation give some information about the distribution, but lack nuance. While the covariance matrix contains more information, it is hard to visualize and interpret.

An alternative method of characterizing a distribution is in terms of representative points, S_X , that are chosen to minimize some loss between X and S_X . We say S_X are exemplars if $S_X \subset X$, and prototypes if $S_X \not\subset X$. For example, support points [18] are a finite set S of prototypes that minimize the energy distance between X and S ; projected support points [21] extend this idea to minimize maximum mean discrepancy [13]. The K -means algorithm can be interpreted as finding a set S_X of prototypes that minimizes the Wasserstein-2 distance between X and S [22]. The K -medoids algorithm [17] behaves similarly, with the added constraint that the representative points S_X be exemplars, i.e. belong to X . Set cover approaches [23] aim to find a set of exemplars S_X so that every $x \in X$ is within some distance ϵ of an exemplar. Such sets of representative points can be augmented with examples representing the extrema of a distribution: for example the MMD-critic algorithm of [16] first selects exemplars that minimize the estimated MMD between X and S_X , and then selects ‘‘critics’’ of these exemplars, which are points in X that are poorly explained by S_X . Such an approach is particularly helpful if we wish to use the representative points to contrast two classes.

In addition to the general-purpose summarizations described above, there are a number of model-based summarization methods appropriate for specific domains. For example, topic models [24] represent documents as admixtures of distributions over words, that are often semantically interpretable. Document summarization methods [25] aim to provide human-readable summaries of documents, and movie summarization methods [26] reduce videos to a set of summary scenes. In this paper, we focus on general-purpose summarization, however extension of the concept to domain-specific algorithms is an interesting avenue for future research.

2.2 Measuring distributional distances and data drift

The idea of measuring and quantizing the difference between two distributions, based on samples from those distributions, dates back to the earliest days of hypothesis testing [27]. Two-sample tests measure the difference between some statistic s evaluated on X and Y (for example, the mean or the empirical CDF), and consider it’s magnitude with respect to the null distribution. As a recent example, consider the kernel two-sample test, which estimates the maximum mean discrepancy (MMD) between two distributions [13]. The MMD between \mathbb{P} and \mathbb{Q} is given by

$$\text{MMD}(\mathbb{P}, \mathbb{Q}) = \sup_{f \in \mathcal{F}} [\mathbb{E}_{\mathbb{P}} f(X) - \mathbb{E}_{\mathbb{Q}} f(Y)]^2$$

where \mathcal{F} is the space of all functions in the unit-ball of a universal RKHS. $\text{MMD}(\mathbb{P}, \mathbb{Q}) \geq 0$, with the equality holding only if $\mathbb{P} = \mathbb{Q}$. We can estimate $\text{MMD}(\mathbb{P}, \mathbb{Q})$ from samples $X \sim \mathbb{P}, Y \sim \mathbb{Q}$ as

$$\widehat{\text{MMD}}(X, Y) = \frac{1}{N(N-1)} \sum_{i=1}^N \sum_{j=1}^N k(x_i, x_j) + \frac{1}{M(M-1)} \sum_{i=1}^M \sum_{j=1}^M k(y_i, y_j) - \frac{2}{NM} \sum_{i=1}^N \sum_{j=1}^M l(x_i, y_j)$$

We can estimate distribution of $\widehat{\text{MMD}}(X, Y)$ under the null distribution that $\mathbb{P} = \mathbb{Q}$ either via sampling or parametric approximations, and use this null distribution to determine whether the distance between the two distributions is statistically significant.

We can extend the idea of a two-sample test to the more general setting, where we are interested in knowing whether a distribution is changing over time. This is known as data drift or concept drift. Detecting data drift is an important task when using machine learning algorithms in production: if the model learned at time t does not capture relationships present at time t' , or if it lacks training examples typical of the distribution at time t' , its performance at time t' will be suboptimal. Distributional distances such as MMD [28], total variation [9] and Hellinger distance [9] have been used to measure

the drift magnitude. Looking at such metrics, or at deterioration in model performance [1, 29], can allow us to test whether drift has occurred and to describe its rate [9]. However, such one-dimensional metrics do not always offer much insight into *how* the distributions differ. In a low-dimensional setting, looking at differences in the marginal distributions, either by plotting histograms or comparing summary statistics, can offer insights into the drift—for example, telling us that the proportion of men has increased, but the average age has decreased. Such naive visualizations ignore higher-order correlations, however: If the average age of men increased, but the average age of women decreased, we may not see any difference in the marginal distributions. Scatter plots allow us to look at pairwise correlations, but the number of such plots may be large. Further, as we discussed in Section 2.1, such marginal distributions may not be easily interpretable.

A number of authors have sought to provide more interpretable representations of data drift. [14] provide a visualization method based on sequences of histograms; however this is only appropriate for relatively low-dimensional data. [14] provide a visualization method based on sequences of histograms; however this is only appropriate for relatively low-dimensional data. [15] provide a more flexible collection of visualization methods, that includes histograms and low-dimensional embeddings. [8] introduce the idea of a "concept drift map", which plots the both the overall drift magnitude, and the marginal drift magnitude. This allows some insight into which variables are responsible for the drift, but as before it will suffer when the drift is mostly apparent in the correlation structure. Further, it only conveys the magnitude, rather than the direction of the drift. Taking a different tack, [30] and [31] aim to detect changes to the conditional distribution $P(Y|X)$, using the Interactions-based Method for Explanations [32] to estimate the contribution of each example's attribute values to the example's class label. Differences in explanations suggest a difference in the conditional class probability.

3 Characterizing related data sets using ANOVA exemplars

As described in Section 2.1, we can generate representative points S_X for a dataset X by minimizing some distance d between X and S_X ,

$$S_X = \arg \min_{S \in \mathcal{S}_K} d(X, S). \quad (1)$$

Here, \mathcal{S}_K is the space of all size- K sets of either exemplars or prototypes. In this paper, we focus on the exemplar setting, where S_X is constrained to be a subset of some set of real exemplars (which could be X , or a super-set of X). We can use any distance d that can be estimated between two sets of observations. For example, k -medioids exemplars minimize the sum of within-cluster variances [17]; support points minimize energy distance [18]; the exemplar component of MMD-critic minimizes MMD [16].

Our goal is to jointly find exemplars S_X and S_Y for two datasets X and Y , in a manner that allows us to directly compare S_X and S_Y (and by extension, X and Y). Directly applying Equation 1 to find exemplars separately for both X and Y will ensure that the exemplars are representative, but they will not necessarily be easy to compare: in general, S_X and S_Y will have no points in common (even if they are selecting from the same set of candidate exemplars \mathcal{S}).

To aid the user in interpreting the difference between S_X and S_Y , we add a penalty term to our optimization problem, so that

$$S_X, S_Y = \arg \min_{R, S} \mathcal{L}_\lambda(X, Y, R, S) := d(X, R) + d(Y, S) - \lambda |R \cap S|. \quad (2)$$

Here, we are encouraging S_X and S_Y to overlap. The result is three sets of exemplars, S_X^ℓ , S_Y^ℓ and S_{XY}^s , such that

$$\begin{aligned} S_X &= S_X^\ell \cup S_{XY}^s \\ S_Y &= S_Y^\ell \cup S_{XY}^s \end{aligned}$$

This decomposition of exemplars into a shared component S_{XY}^s and local components S_X^ℓ, S_Y^ℓ is reminiscent of the classical ANOVA decomposition, motivating the name ANOVA exemplars. The shared exemplars S_{XY}^s represent commonalities between the distributions, or examples of data points that are representative of either data set. The local exemplars S_X^ℓ, S_Y^ℓ represent examples of data sets that are only representative of one of the two data sets.

Such a representation provides a clear way of characterizing the difference between the two distributions. S_X^ℓ provides direct examples of the type of data points that are over-represented in X , and S_Y^ℓ provides direct examples of the type of data points that are over-represented in Y .

3.1 A greedy algorithm for finding ANOVA exemplars

To find a local minimum of Equation 2, we iterate through a series of local swaps, selected randomly from the following options:

- **local replacement:** Replace an exemplar $s \in S_X^\ell$ (or equivalently S_Y^ℓ) with $s^* = \arg \min_{s^* \in (S \setminus S_X) \cup \{s\}} \mathcal{L}_\lambda(X, Y, (S_X \setminus s) \cup s^*, S_Y)$.
- **shared replacement:** Replace an exemplar $s \in S_{XY}^s$ with $s^* = \arg \min_{s^* \in (S \setminus (S_X \cup S_Y)) \cup \{s\}} \mathcal{L}_\lambda(X, Y, (S_X \setminus s) \cup s^*, (S_Y \setminus s) \cup s^*)$.
- **merge:** Replace an exemplar $s \in S_X^\ell$ (or equivalently S_Y^ℓ) with $s^* = \arg \min_{s^* \in (S_Y \setminus S_X) \cup \{s\}} \mathcal{L}_\lambda(X, Y, (S_X \setminus s) \cup s^*, S_Y)$.
- **split:** Replace an exemplar $s \in S_{XY}^s$ with two exemplars $r^*, s^* = \arg \min_{r^* \in (S \setminus S_X) \cup s, s^* \in (S \setminus S_Y) \cup s} \mathcal{L}_\lambda(X, Y, (S_X \setminus s) \cup r^*, (S_Y \setminus s) \cup s^*)$.

Each step scales quadratically with the larger of the two datasets. While the lack of convexity means that this procedure is not guaranteed to find a global optimum, in practice we find it obtains good-quality local optima. If desired, the procedure can be repeated to give multiple candidate local optima.

4 Evaluation

4.1 Qualitative analysis on synthetic data

We begin by showing examples of ANOVA exemplars on synthetic data, to visualize the behavior of our algorithm. We generated five cluster means $\mu_i \sim \text{Normal}(0, \mathbf{I})$, and two probability vectors π_X, π_Y according to a standard Dirichlet distribution. We used these to generate two datasets X and Y , each of 1000 points, from Gaussian mixture models with cluster centers μ_i , covariances $0.1\mathbf{I}$ and cluster probabilities π_X and π_Y respectively. We show the two datasets in Figure 2a.

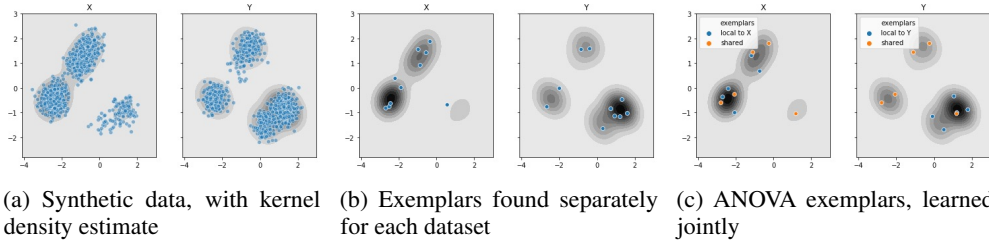


Figure 2: MMD exemplars, and ANOVA exemplars, on two related synthetic datasets.

In Figure 2b we show the exemplars found according to Equation 1, using the greedy algorithm described by [16]. In Figure 2c we show the ANOVA exemplars found using our algorithm, with $\lambda = 0.01$. While both sets of exemplars are good fits for the data, the ANOVA exemplars capture the commonality between the two distributions.

4.2 Analysis on real-world datasets with data drift

Next, we consider two real-world datasets.

Yearbook: A collection of images of faces taken from yearbooks between 1900 and 1982 [33]. We generated 512-dimensional embeddings of the 15367 female, front-facing photographs using the torchvision pre-trained implementation of ResNet [34]. We reduced the dimension using PCA to capture 95% of the original variance, resulting in 201-dimensional representations. We partitioned the data into decades, and created ANOVA exemplars for each pair of decades.

NeurIPS: a collection of abstracts taken from NeurIPS papers from 1987 to 1917.¹ We generated 768-dimensional embeddings using the uncased, pre-trained version of SciBERT [35]. We reduced the dimension using PCA, as before, resulting in 198-dimensional representations. We partitioned the data by year, and created ANOVA exemplars for each pair of decades.

In each case, we collected $M = 10$ exemplars, used a sum of squared exponential kernels, $k = \sum_i \exp\{\|x - x'\|^2 / 2\sigma_i^2\}$, with $\sigma = (1, 2, 4, 8, 16)$, as suggested by [36]. We ran our algorithm for ten iterations, with five random restarts. To set λ , we first found M exemplars for each dataset using the greedy algorithm of [16], and looked at the average MMD between exemplars for different datasets, d . We set $\lambda = \bar{d} / 2M$.

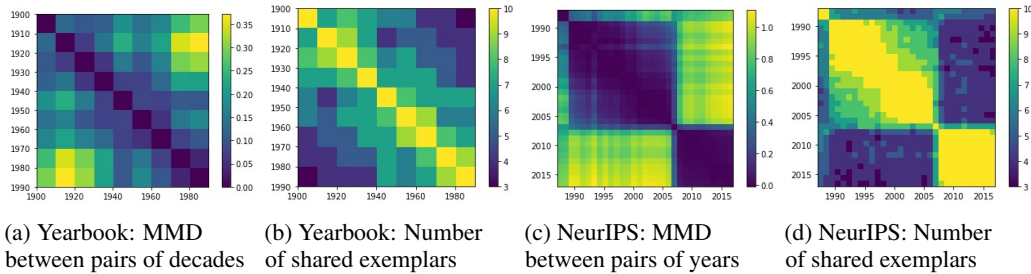


Figure 3: Comparing MMD between different time points (a, c) with the number of shared exemplars between different time points (b, d).

Figures 3a and 3c quantify the magnitude of data drift in each dataset, by looking at the estimated MMD between time periods. We see that the yearbook photos vary gradually across time, while the NeurIPS abstracts show a dramatic change around 2007, coinciding with the birth of Deep Learning. Compare these estimates with the number of $|S_{XY}^s|$ of shared support points, shown in Figures 3b and 3d. We see pairs of time points with low MMD have a large number of exemplars in common, and pairs with higher MMD have fewer shared exemplars.



(a) Exemplars for photos from the 1910s and 1930s. (b) Exemplars for photos from the 1950s and 1970s. Top: Local to 1910s. Middle: Shared. Bottom: Local to 1930s. Top: Local to 1950s. Middle: Shared. Bottom: Local to 1970s.



(c) Exemplars for photos from the 1920s and 1980s. Top: Local to 1920s. Middle: Shared. Bottom: Local to 1980s.

Figure 4: ANOVA exemplars for yearbook photos.

A subset of the exemplars for the yearbook dataset are shown in Figure 4, with the full collection included in the appendix. We see that the earlier decades tend to have exemplars with shorter, curlier hair. In Table 1 we show the titles of papers selected as ANOVA exemplars for the years 2005 and

¹<https://www.kaggle.com/benhamner/nips-papers>

Table 1: ANOVA exemplars for NeurIPS papers

<p>Local to 2005</p>	<p>Generalization in Clustering with Unobserved Features (2005) Evidence Optimization Techniques for Estimating Stimulus-Response Functions (2002) Robust design of biological experiments (2005) Efficient Unsupervised Learning for Localization and Detection in Object Categories (2005) Sequence and Tree Kernels with Statistical Feature Mining (2005) Walk-Sum Interpretation and Analysis of Gaussian Belief Propagation (2005)</p>
<p>Shared</p>	<p>Learning on graphs using Orthonormal Representation is Statistically Consistent (2014) Ordered Classes and Incomplete Examples in Classification (1996) Sparse Gaussian Processes using Pseudo-inputs (2005) Discriminative State Space Models (2017)</p>
<p>Local to 2017</p>	<p>Population Matching Discrepancy and Applications in Deep Learning (2017) Partial Hard Thresholding: Towards A Principled Analysis of Support Recovery (2017) Prototypical Networks for Few-shot Learning (2017) Self-Supervised Intrinsic Image Decomposition (2017) Equilibrated adaptive learning rates for non-convex optimization (2015) Probabilistic Rule Realization and Selection (2017)</p>

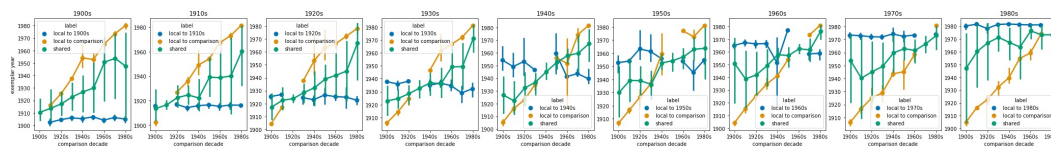


Figure 5: Years of exemplars in S_t^ℓ , $S_{t'}^\ell$ and $S_{t'}^s$ for yearbook photos from different decades.

2017. The exemplars local to 2017 cover modern research techniques such as deep learning; the exemplars local to 2005 cover topics such as message passing algorithms and unsupervised learning. In the shared space, we have some theory-focused papers that are less tied to a specific time period, and topics such as sparse Gaussian processes that span both eras.

To get a more quantitative impression of the quality of the shared and local exemplars, we can look at the dates associated with them. As we saw in Figure 3, both datasets exhibit temporal drift. We would expect that, for when looking at exemplars S_t^ℓ , $S_{t'}^s$ and $S_{t'}^\ell$ representing data X_t and $X_{t'}$, that exemplars S_t^ℓ and $S_{t'}^\ell$ would tend to contain data points from times t and t' , respectively, and that exemplars $S_{t'}^s$ would tend to contain data points from in between these time periods. In Figure 5 we plot the years of the exemplars for each pair of decades. We see that, as expected, the local exemplars tend to belong to the decade in question, while the shared exemplars span a range of decades. Similarly, in Figure 6 we plot the years of the exemplars for the NeurIPS data, for all possible year-year pairs. Again, we see that the local exemplars tend to belong to years close to the target years, while the shared exemplars span a range of years.

Finally, in Table 2 we look at the MMD between a data point and various exemplars or subsets of exemplars. We first consider MMD exemplars [16] S_t^{MMD} trained separately on each time period. The first two columns show the average value of $d(X_t, S_t^{\text{MMD}})$ (i.e. the difference (in terms of MMD) between the data at time point t , and the exemplars for that time point) and the average value of $d(X_t, S_{t' \neq t}^{\text{MMD}})$ (i.e. the average difference between the data at time point t , and exemplars from time point $t' \neq t$). The next two columns show the average distances between the full set ($S_t = S_t^\ell \cup S_{t'}^s$)

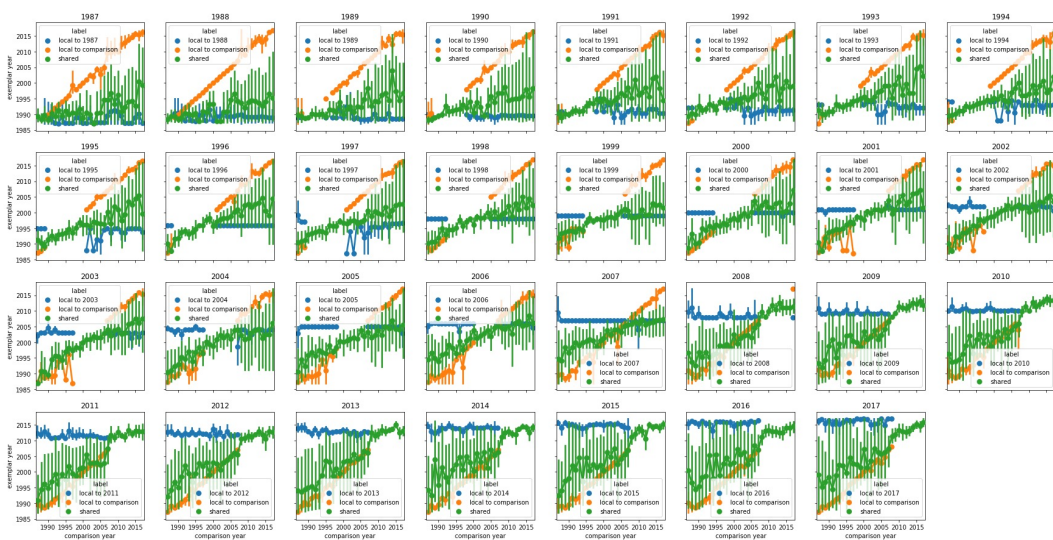


Figure 6: Years of exemplars in S_t^ℓ , $S_{t'}^\ell$ and $S_{tt'}^s$ for NeurIPS from different years.

of ANOVA exemplars obtained by jointly learning $d(X_t, S_t)$ and $d(X_t, S_{t' \neq t})$ on two different time steps. We see that the distances are comparable to those obtained without encouraging overlap, indicating that the ANOVA exemplars are of similar quality.

Next, we see the decomposition of those ANOVA exemplars into $d(X_t, S_t^\ell)$, $d(X_t, S_{tt'}^s)$, and $d(X_t, S_{t'}^\ell)$. We see that, on average, the shared exemplars are close to both datasets, while the local exemplars are close to their local dataset, but far from the contrasting dataset.

Table 2: Average distances (in terms of MMD) between data at each time point, and exemplars at the same and different time points.

	$d(X_t, S_t^{\text{MMD}})$	$d(X_t, S_{t' \neq t}^{\text{MMD}})$	$d(X_t, S_t)$	$d(X_t, S_{t' \neq t})$
Yearbook	-0.06364 (0.005599)	0.1095 (0.09008)	-0.06263 (0.005643)	0.06993 (0.08732)
NeurIPS	-0.1882 (0.02271)	0.02724 (0.1903)	-0.1653 (0.02467)	-0.04599 (0.1424)

dataset	$d(X_t, S_t^\ell)$	$d(X_t, S_{tt'}^s)$	$d(X_t, S_{t'}^\ell)$
Yearbook	-0.03848 (0.05848)	-0.04366 (0.02199)	0.2865 (0.1255)
NeurIPS	-0.1366 (0.3035)	-0.1492 (0.07110)	0.6800 (0.4703)

5 Conclusion

ANOVA exemplars offer a new method for summarizing related datasets. By identifying areas of shared and local support, these exemplars can be used to understand differences and similarities between datasets, making them well-suited to analysing data in the presence of potential data drift, or comparing two similar datasets.

In this paper, we used MMD as the distance between distributions and exemplars; however a number of choices could be made. The development of ANOVA-type variants of other summary algorithms is an interesting avenue for future work.

Broader Impact

There is an increasing push for greater understanding and explainability of both algorithms and datasets [37, 38], and exemplars have been proposed as a way of increasing understanding of datasets [16]. Our work extends this idea, using exemplars to aid in understanding of data drift. We hope that it will prove useful in ensuring practitioners understand their data and how it evolves, leading to better performance of ensuing algorithms.

A concern with the exemplar framework is that it returns real data points. This could be problematic if the individual data contain sensitive explanations. Moving to a prototype framework would help mitigate this risk, albeit at a greater computational cost. We hope to see exploration of this direction in future work.

References

- [1] Joao Gama, Pedro Medas, Gladys Castillo, and Pedro Rodrigues. Learning with drift detection. In *Brazilian Symposium on Artificial Intelligence*, pages 286–295, 2004.
- [2] Kyosuke Nishida and Koichiro Yamauchi. Detecting concept drift using statistical testing. In *International Conference on Discovery Science*, pages 264–269, 2007.
- [3] Albert Bifet and Ricard Gavaldà. Learning from time-changing data with adaptive windowing. In *International Conference on Data Mining*, pages 443–448, 2007.
- [4] Daniel Kifer, Shai Ben-David, and Johannes Gehrke. Detecting change in data streams. In *Conference on Very Large Data Bases*, volume 4, pages 180–191, 2004.
- [5] Xiuyao Song, Mingxi Wu, Christopher Jermaine, and Sanjay Ranka. Statistical change detection for multi-dimensional data. In *International Conference on Knowledge Discovery and Data Mining*, pages 667–676, 2007.
- [6] Abdulhakim A Qahtan, Basma Alharbi, Suojin Wang, and Xiangliang Zhang. A PCA-based change detection framework for multidimensional data streams: Change detection in multi-dimensional data streams. In *International Conference on Knowledge Discovery and Data Mining*, pages 935–944, 2015.
- [7] Feng Gu, Guangquan Zhang, Jie Lu, and Chin-Teng Lin. Concept drift detection based on equal density estimation. In *International Joint Conference on Neural Networks*, pages 24–30, 2016.
- [8] Geoffrey I Webb, Loong Kuan Lee, Bart Goethals, and François Petitjean. Analyzing concept drift and shift from sample data. *Data Mining and Knowledge Discovery*, 32(5):1179–1199, 2018.
- [9] Geoffrey I Webb, Roy Hyde, Hong Cao, Hai Long Nguyen, and François Petitjean. Characterizing concept drift. *Data Mining and Knowledge Discovery*, 30(4):964–994, 2016.
- [10] J Zico Kolter and Marcus A Maloof. Dynamic weighted majority: An ensemble method for drifting concepts. *Journal of Machine Learning Research*, 8(Dec):2755–2790, 2007.
- [11] Stephen H Bach and Marcus A Maloof. Paired learners for concept drift. In *International Conference on Data Mining*, pages 23–32, 2008.
- [12] Heitor M Gomes, Albert Bifet, Jesse Read, Jean Paul Barddal, Fabrício Enembreck, Bernhard Pfahringer, Geoff Holmes, and Talel Abdesslem. Adaptive random forests for evolving data stream classification. *Machine Learning*, 106(9-10):1469–1495, 2017.
- [13] Arthur Gretton, Karsten M Borgwardt, Malte J Rasch, Bernhard Schölkopf, and Alexander Smola. A kernel two-sample test. *Journal of Machine Learning Research*, 13(Mar):723–773, 2012.
- [14] Kevin B Pratt and Gleb Tschapek. Visualizing concept drift. In *ACM SIGKDD International Conference on Knowledge Discovery and Data Mining*, pages 735–740, 2003.

- [15] Fred Hohman, Kanit Wongsuphasawat, Mary Beth Kery, and Kayur Patel. Understanding and visualizing data iteration in machine learning. In *CHI Conference on Human Factors in Computing Systems*, pages 1–13, 2020.
- [16] Been Kim, Rajiv Khanna, and Oluwasanmi O Koyejo. Examples are not enough, learn to criticize! criticism for interpretability. In *Advances in Neural Information Processing Systems*, pages 2280–2288, 2016.
- [17] Leonard Kaufmann and Peter Rousseeuw. Clustering by means of medoids. *Data Analysis based on the L1-Norm and Related Methods*, pages 405–416, 01 1987.
- [18] Simon Mak and V Roshan Joseph. Support points. *The Annals of Statistics*, 46(6A):2562–2592, 2018.
- [19] Robert G Alexander, Joseph Schmidt, and Gregory J Zelinsky. Are summary statistics enough? evidence for the importance of shape in guiding visual search. *Visual Cognition*, 22(3-4): 595–609, 2014.
- [20] Tim Lauer, Tim HW Cornelissen, Dejan Draschkow, Verena Willenbockel, and Melissa L-H Vö. The role of scene summary statistics in object recognition. *Scientific Reports*, 8(1):1–12, 2018.
- [21] Simon Mak and V Roshan Joseph. Projected support points: a new method for high-dimensional data reduction. *arXiv preprint arXiv:1708.06897*, 2017.
- [22] David Pollard. Quantization and the method of k-means. *IEEE Transactions on Information theory*, 28(2):199–205, 1982.
- [23] Jacob Bien and Robert Tibshirani. Prototype selection for interpretable classification. *The Annals of Applied Statistics*, pages 2403–2424, 2011.
- [24] David M Blei, Andrew Y Ng, and Michael I Jordan. Latent Dirichlet allocation. *Journal of Machine Learning Research*, 3(Jan):993–1022, 2003.
- [25] Hui Lin and Jeff Bilmes. A class of submodular functions for document summarization. In *Association for Computational Linguistics: Human Language Technologies*, pages 510–520, 2011.
- [26] Chong-Wah Ngo, Yu-Fei Ma, and Hong-Jiang Zhang. Video summarization and scene detection by graph modeling. *IEEE Transactions on Circuits and Systems for Video Technology*, 15(2): 296–305, 2005.
- [27] John Arbuthnot. Ii. an argument for divine providence, taken from the constant regularity observ’d in the births of both sexes. *Philosophical Transactions of the Royal Society of London*, 27(328):186–190, 1712.
- [28] Stephan Rabanser, Stephan Günemann, and Zachary Lipton. Failing loudly: an empirical study of methods for detecting dataset shift. In *Advances in Neural Information Processing Systems*, pages 1394–1406, 2019.
- [29] Shujian Yu, Zubin Abraham, Heng Wang, Mohak Shah, Yantao Wei, and José C Príncipe. Concept drift detection and adaptation with hierarchical hypothesis testing. *Journal of the Franklin Institute*, 356(5):3187–3215, 2019.
- [30] Jaka Demšar, Zoran Bosnić, and Igor Kononenko. Visualization and concept drift detection using explanations of incremental models. *Informatica*, 38(4), 2014.
- [31] Jaka Demšar and Zoran Bosnić. Detecting concept drift in data streams using model explanation. *Expert Systems with Applications*, 92:546–559, 2018.
- [32] Erik Štrumbelj, Igor Kononenko, and M Robnik Šikonja. Explaining instance classifications with interactions of subsets of feature values. *Data & Knowledge Engineering*, 68(10):886–904, 2009.

- [33] Shiry Ginosar, Kate Rakelly, Sarah Sachs, Brian Yin, and Alexei A Efros. A century of portraits: A visual historical record of American high school yearbooks. In *IEEE International Conference on Computer Vision Workshops*, pages 1–7, 2015.
- [34] Kaiming He, Xiangyu Zhang, Shaoqing Ren, and Jian Sun. Deep residual learning for image recognition. In *Computer Vision and Pattern Recognition*, pages 770–778, 2016.
- [35] Iz Beltagy, Kyle Lo, and Arman Cohan. SciBERT: Pretrained language model for scientific text. In *Empirical Methods in Natural Language Processing*, 2019.
- [36] Chun-Liang Li, Wei-Cheng Chang, Yu Cheng, Yiming Yang, and Barnabás Póczos. MMD GAN: Towards deeper understanding of moment matching network. In *Advances in Neural Information Processing Systems*, pages 2203–2213, 2017.
- [37] Timnit Gebru, Jamie Morgenstern, Briana Vecchione, Jennifer Wortman Vaughan, Hanna Wallach, Hal Daumé III, and Kate Crawford. Datasheets for datasets. In *Workshop on Fairness, Accountability, and Transparency in Machine Learning*, 2018.
- [38] Kacper Sokol and Peter Flach. Explainability fact sheets: a framework for systematic assessment of explainable approaches. In *Conference on Fairness, Accountability, and Transparency*, pages 56–67, 2020.

A Additional exemplars

In this section, we include additional examples of ANOVA exemplars from the yearbook dataset. Additional examples from the NeurIPS dataset can be found in the accompanying notebooks, which will be published on github upon publication.



(a) 1900s vs 1910s



(b) 1900s vs 1920s



(c) 1900s vs 1930s



(d) 1900s vs 1940s



(e) 1900s vs 1950s



(f) 1900s vs 1960s



(g) 1900s vs 1970s



(h) 1900s vs 1980s



(i) 1910s vs 1920s



(j) 1910s vs 1930s



(k) 1910s vs 1940s



(l) 1910s vs 1950s

Figure 7: ANOVA exemplars for yearbook photos. In each case: Top row = local to earlier year, middle row = shared, bottom row = local to later year.



(a) 1910s vs 1960s



(b) 1910s vs 1970s



(c) 1910s vs 1980s



(d) 1920s vs 1930s



(e) 1920s vs 1940s



(f) 1920s vs 1950s



(g) 1920s vs 1960s



(h) 1920s vs 1970s



(i) 1920s vs 1980s



(j) 1930s vs 1940s



(k) 1930s vs 1950s



(l) 1930s vs 1960s



(m) 1930s vs 1970s



(n) 1930s vs 1980s

Figure 8: ANOVA exemplars for yearbook photos. In each case: Top row = local to earlier year, middle row = shared, bottom row = local to later year.



(a) 1940s vs 1950s



(b) 1940s vs 1960s



(c) 1940s vs 1970s



(d) 1940s vs 1980s



(e) 1950s vs 1960s



(f) 1950s vs 1970s



(g) 1950s vs 1980s



(h) 1960s vs 1970s



(i) 1960s vs 1980s



(j) 1970s vs 1980s

Figure 9: ANOVA exemplars for yearbook photos. In each case: Top row = local to earlier year, middle row = shared, bottom row = local to later year.